

Design and Analysis of Amphibious Flying Wing UAV

Sameer Makthal¹, Sai Dinesh², Muhammad Tabish³

^{1, 2, 3} Department of Mechanical Engineering,
Sreenidhi Institute of Science and Technology
Hyderabad, India

Abstract—This Drones are proving to be an integral part of today's engineering works with applications in military systems, delivery services, emergency relief, geographic and oceanographic mapping and evacuation, among others. A simple drone is an unmanned aerial vehicle designed for flight with one or more propellers and controlled remotely through an RC.

An amphibious drone is a UAV capable of being maneuvered in air across certain altitudes as well as through water till a certain depth. Development of an unmanned amphibious vehicle integrating the features of a multi-rotor UAV with a submerging mechanism that can perform functions such as surveillance, mapping and study of environments inaccessible to humans, is the present aim of the study. The design of the drone body, wings and components of the amphibious drone were developed with due consideration for aerodynamic, structural, and environmental aspects in air as well as water.

To develop the said UAV for listed applications, payload, dynamic flight effects and dimensional calculations are done, based on which analysis such as performance analysis and stability analysis was performed on XFLR5 for different Air foils and winglets. With the air foil structure the wings and plane body were designed on the software. Further development of the CAD model is carried on the SOLIDWORKS software completing the detailed CAD model. With two different operating conditions, the loads acting on the UAV have been considered and thorough structural analysis has been performed on the support structures of the wing. Required calculations, research and analysis has been performed with an aim to develop a prototype.

Keywords—Amphibious; UAV; aerodynamic; payload; foils; CAD; structural.

I. INTRODUCTION

The use of unmanned vehicles, including Unmanned Aerial Vehicles (UAVs) and Unmanned Underwater Vehicles (UUVs), has expanded greatly in recent years, motivated by myriad commercial and military applications. While developments have advanced the capabilities of both aerial and underwater vehicle classes, a single vehicle capable of performing in both the aerial and underwater domains has remained elusive and haven't been explored much. There has been significant interest in developing a cross-domain vehicle capable of operating seamlessly both underwater and in the air. However, no previous vehicle has offered a fully functional design capable of repeated transitions between domains, low-energy loitering, and useful levels of endurance. Such a cross-domain vehicle concept would merge the benefits of operating in each of these domains, combining the persistence of a surface vehicle, the diving, underwater

manoeuvring, and stealth capabilities of an underwater vehicle, and the speed and range of an airborne vehicle. The cross-domain concept of operations thus greatly increases the range of sensing modality, communication methods, and mission scenarios available to the vehicle.

Unmanned underwater vehicle is a kind of drone which can operate underwater remotely controlled by human. A drone with this capability gives a big hand to the related field to carry out some dangerous mission underwater. There are two categories under this UUV drone, which are Remotely Operated Underwater Vehicles (ROVs) and Autonomous Underwater Vehicles (AUVs).

Development of an unmanned amphibious vehicle integrating the features of a multi-rotor UAV and a plane with a certain air-foil is the focus of the present study. Components and design of the amphibious vehicle are developed with due consideration for aerodynamic, structural, and environmental aspects. Starting with the payload and parameter calculations the wing design and analysis are carried out in XFLR5 software. Finite element analysis (FEA) on static thrust conditions and skirt pressure are performed to evaluate the strength of the structure. For diverse wind conditions and angles of attack (AOA), computational fluid dynamic (CFD) analysis is carried out to assess the effect of drag and suitable design modification is suggested.

II. DESIGN AND DEVELOPMENT OF AMPHIBIOUS UAV - A LITERATURE REVIEW

UAVs are becoming progressively conventional in today's engineering. Many of these have vertical take-off and landing capability, especially the quad copter type. UAV's were first developed to gain an advantage in war during the world-war era, each country devoted its own technology in its development. Non-military drone use began in earnest in 2006. Government agencies for disaster relief, border surveillance and wildfire fighting, while corporations began using drones to inspect pipelines and spray pesticides on farms and lots of other job were made easier and safer with drone use.

New flying wing design was developed at the Unmanned Systems Lab (USL) at Virginia Tech to serve delivery and remote sensing. The fully autonomous unmanned aerial vehicle (UAV), named EcoSoar was developed in such a way that local fabrication, operation, and maintenance of the aircraft are all possible. In order to present a competitive

financial model. In order to be a viable solution in the developing world, EcoSoar utilizes customizable 3D-printed parts and wings made from cheap materials like poster board and packing tape.

With further development and possibilities, the amphibious drone was developed to sustain flight in air as well as dip into water to a certain depth. In order to move through water, buoyancy force needs to be balanced and it challenges the structural integrity, it must have a better communication system with more penetration and less attenuation of the signal. The aluminium alloy is used as a rebar structure to support the outer shielding and support excessive loads when venturing into environments of heavy pressure and drag. Further, use of carbon fibre composites as spars to support ribs and a carbon fibre composite as the outer structure to facilitate weight reduction and increase strength. Based on above considerations the amphibious drone has been developed and measuring their efficiency in both air and water while closely monitoring their functional efficiency for further applications. Applications such as coastal rescue, surveillance, oceanographic research, geographic and oceanographic mapping etc.

Weisler et al. (2017) conducted a research on performance characterization of the first fixed-wing unmanned aerial vehicle capable of cross domain operation in both aerial and underwater environments with low-energy loitering abilities. Wesiler et al. (2017) described a passive flooding mechanism that enabled transition of UAV from aerial flight to underwater travel. This mechanism of flooding is similar in principle to that of a submarine, but William Stewart et al. (2019) thoroughly described the efficiency of this passive flooding technique and how the flooding and draining of a wing tank is performed in a short period of time. The research successfully developed a functioning amphibious prototype, but its functionality was restricted as it carried no payload of any type.

Communication with the UAV once it has transitioned into underwater flight is vital to perform required tasks and gain required signals. As the UAV dives deeper there are chances of losing radio signals and increasing its attenuation. R. Suresh et al. (2020) addressed this very issue of communications through installation of a positioning module on the UAV to determine its position underwater and install a static ground communications station. Though this seems to be a viable option, installation of a ground station restricts the portability of the amphibious drone. With the installation of a visual communication device i.e. a camera onto the drone itself, issues of positioning and travel can be eliminated. Further, use of stronger comms device and a dedicated module for amplifying radio signals between the UAV and its controller remains to be the perfect solution.

As mentioned earlier, the primary motive behind designing an amphibious drone is surveillance and mapping of two different environments through a single device. W. H. Wang et al. (2008) designed and developed an unmanned underwater vehicle for shallow water tasks. The material used were in accordance to its region and depth of application. The UUV was fitted with sensors for temperature and depth. As the

drone was developed for underwater travel only, citing this paper, amongst others, data and methods can be referred to, for the development of an Unmanned Amphibious Vehicle.

Design of air foils remains an important aspect of any aerial vehicle design, definite calculations must be performed to determine the structure and design of air foil to be used based on the vehicle design and flying conditions. Air foil calculators such as air foil tools, an online site that documents all characteristics and performance parameters of every available air foil, is a good starting point. Further air foil design is developed in software such as XFLR5 with due analysis carried on them to meet our needs and suit our applications.

XFLR5 is an analysis tool for air foils, wings and planes operating at low Reynolds Numbers. It includes: XFoil's Direct and Inverse analysis capabilities. Wing design analysis capabilities based on the Lifting Line Theory, on the Vortex Lattice Method, and on a 3D Panel Method. Knowing that our designed UAV is designed to operate at low Re numbers, this software is the perfect choice to design, analyse and gauge the UAV.

III. OBJECTIVE

Every new era demands a new development and advancement in technology. It demands technology that helps us conquer not just in one domain but in multiple fields.

UAVs have been under development since the start of 21st century, gaining huge break-through in this past decade. With their usefulness proved in many sectors including communication, surveillance and majorly defense.

We're further looking to develop the existing drone technology to avail them for aerial as well as underwater traversal. This cross-domain vehicle 'The Amphibious drone' will be able to transition between air and water seamlessly with full functionality in both.

A. Need for an Amphibious Drone

With the air domain captured and swayed but the UAVs and the underwater work handled by the AUVs and ROVSs there is a need for an autonomous vehicle to be able to operate and handle both the environment, thus the development of an Amphibious drone came to. This ability of the drone to traverse and change its environment could be applied in any field that requires a drone use. The defense sector could hugely benefit from such a vehicle, with its underwater maneuvering capabilities, stealth useful for dangerous missions while not losing any ground on the aerial front with its flight abilities.

B. Performance requirements

While starting with the design of the drone, its performance requirements- its limits and access have been defined.

1) The Air Travel requirements include

- Mean flight altitude
- Maximum altitude
- Velocity

- Air travel time
 - Control distance
- 2) *Underwater Requirements*
- Density range of water, Reynolds number
 - Depth of water
 - Ingress and egress mechanism
 - Overall dynamic stability

C. Equations

The equations are an exception to the prescribed specifications of this template. You will need to determine whether or not your equation should be typed using either the Times New Roman or the Symbol font (please no other font). To create multileveled equations, it may be necessary to treat the equation as a graphic and insert it into the text after your paper is styled.

Number equations consecutively. Equation numbers, within parentheses, are to position flush right, as in (1), using a right tab stop. To make your equations more compact, you may use the solidus (/), the exp function, or appropriate exponents. Italicize Roman symbols for quantities and variables, but not Greek symbols. Use a long dash rather than a hyphen for a minus sign. Punctuate equations with commas or periods when they are part of a sentence, as in

$$a + b = \gamma \quad (1)$$

Note that the equation is centered using a center tab stop. Be sure that the symbols in your equation have been defined before or immediately following the equation. Use "(1)," not "Eq. (1)" or "equation (1)," except at the beginning of a sentence: "Equation (1) is ..."

D. Some Common Mistakes

- The word "data" is plural, not singular.
- The subscript for the permeability of vacuum μ_0 , and other common scientific constants, is zero with subscript formatting, not a lowercase letter "o."
- In American English, commas, semi-/colons, periods, question and exclamation marks are located within quotation marks only when a complete thought or name is cited, such as a title or full quotation. When quotation marks are used, instead of a bold or italic typeface, to highlight a word or phrase, punctuation should appear outside of the quotation marks. A parenthetical phrase or statement at the end of a sentence is punctuated outside of the closing parenthesis (like this). (A parenthetical sentence is punctuated within the parentheses.)
- A graph within a graph is an "inset," not an "insert." The word alternatively is preferred to the word "alternately" (unless you really mean something that alternates).
- Do not use the word "essentially" to mean "approximately" or "effectively."

- In your paper title, if the words "that uses" can accurately replace the word using, capitalize the "u"; if not, keep using lower-cased.
- Be aware of the different meanings of the homophones "affect" and "effect," "complement" and "compliment," "discreet" and "discrete," "principal" and "principle."
- Do not confuse "imply" and "infer."
- The prefix "non" is not a word; it should be joined to the word it modifies, usually without a hyphen.
- There is no period after the "et" in the Latin abbreviation "et al."
- The abbreviation "i.e." means "that is," and the abbreviation "e.g." means "for example."

An excellent style manual for science writers is [7].

IV. DESIGN METHODOLOGY

A. Initial Design Input and Parameter Calculation

In order to determine the dimensions of root chord, tip chord and span we have chosen the approach of achieving a specified cubic wing loading. Cubic wing loading is the ratio between the total weight of the airplane to the total wing area. For the amphibious applications we chose a wing loading of 20 – 25 oz/sqft i.e. approximately 20 WCL (wing cube loading)

$$W.L = \frac{\text{Weight(oz)}}{\text{Area(sqft)}} \quad (1)$$

$$W.C.L = \frac{\text{Weight(oz)}}{\text{Area(sqft)}^{1.5}} \quad (2)$$

Multiple iterations of dimensions of the UAV were analysed until the required wing loading was achieved. There are multiple parameters interrelated that eventually provide the final dimensions in correlation to the wing cube loading.

- The initial step is to confirm the dimensions of the root chord of said UAV. In the case of a flying wing UAV, the length of root chord primarily depends upon the components that are to be installed within the body of the UAV. These components include, but are not limited to, the battery, ESC, wiring, pixhawk, extra weights and payload. Now, in an aerial vehicle the balancing of weights and is crucial. Thus, the positioning of the mentioned components is dependent upon the CoG. The CoG determines a plane's static and dynamic stability. Initially the components are placed randomly, and rough length of root chord is found. The final length falls within the initial length as it depends upon the dimensions of the components itself.

- Step two decides the span of the wing. Span is seen as the overall length of the wing measured from one tip chord to the other. Deciding this length depends either upon an aspect ratio or A.R or the wing cube loading. Given the approach, we chose the length of span based on WCL.
- The next step is to decide a suitable taper ratio which consequentially gives the length of tip chord. This ratio is selected based on the function of UAV, the type of wing it utilises, its operating range of Reynolds number and the highest achievable velocity. Accordingly we have chosen a low taper ratio as we have determined the UAV to be a glider type, utilising a flying wing, operating at low Reynolds number with a maximum achievable velocity of 10m/s. A taper ratio is the ratio between root chord and tip chord of the wing.

$$\lambda = \frac{C_{tip}}{C_{root}} \quad (3)$$

- Determining a sweep angle for the flying wing is the step after deciding a suitable taper ratio. Like taper ratio, sweep angle depends upon the same parameters. For a flying wing, a sweep angle acts like a dihedral angle, whose function is to provide stability to the UAV. Though, an excessively large sweep angle is not suitable for a low velocity UAV. Based on these limitations, a low sweep angle lying within 20 to 25 degrees was chosen. Sweep angle is seen as the angle made by the leading and trailing edge of the wing, with the horizontal.

B. Design Considerations and Component Selection

1) *Motor for Propulsion:* The selection of the motor was done based on the thrust to weight ratio required to propel the wing. The thrust-to-weight ratio can be calculated by dividing the thrust (in SI units – in newtons) by the weight (in newtons) of the engine or vehicle and is a dimensionless quantity.

The thrust-to-weight ratio varies continually during a flight. Thrust varies with throttle setting, airspeed, altitude and air temperature. Aircraft with thrust-to-weight ratio greater than 1:1 can pitch straight up and maintain airspeed until performance decreases at higher altitude.

Based on these considerations, T-motor AT2310 2200 kV Brushless DC Motor is chosen in a dual setup. According to the specifications, APC 6*4 is the recommended propeller (The diameter of the propeller is 6 inches and its pitch is 4 inches). Fig 1. is a visual representation of the chosen motor.

This setup would give a thrust of 1141 grams from each motor at 80% throttle. Since two motors will be used, the resultant thrust is 2282 grams. As the total estimated weight of the wing is 1000 grams, the thrust to weight ratio is 2.282:1. This ratio is acceptable for both aerial and underwater traversal.



Fig. 1. T-motor AT2310 2200kV Brushless DC Motor

2) *Servo Motors:* The servo motors are used for the actuation of the control surfaces and the spoilers of the wing. The control surfaces or the ailerons are used to maneuver the wing in the roll and the pitch axes. The spoilers are flaps on the wing which can be opened to drain out water from the inside of the wing when the UAV egresses from water to air. The servo motor should be able to actuate with good responsiveness in air and should be able to overcome water pressure while it is underwater. The servo should also be completely waterproof.

Keeping these considerations in mind, Hitec Multiplex HS-5646WP High Voltage, High Torque, Programmable Digital Waterproof Servo is chosen. 4 of these servos are used to actuate the two ailerons and the two spoilers. Fig 2. shows the selected servo.



Fig. 2. Hitec Multiplex HS - 5646WP high voltage, high torque, programmable digital waterproof servo

3) *Electronic Speed Controller and Battery:* Based on the current drawn by the motor, which is about 26 Amps by each motor on an average, AT 40A ESC is used by each motor.

Based on the ESC and the motors used, 5200mAh 3S 40C/80C Lithium polymer battery Pack (LiPo) is used as the power supply. This setup would give an average flight time of 13 minutes for this prototype.

4) *Transmitter and Receiver:* To pilot this aircraft, mz-12 PRO 12 Channel 2.4GHz HoTT Transmitter with Falcon 12 Receiver is used. Fig 3. shown below is the selected transmitter and receiver.



Fig. 3. Mz-12 PRO 12 channel 2.4GHz HoTT transmitter with Falcon 12 receiver

The receiver connects all the electronics on the aircraft together and receives command from the transmitter. The transmitter is held and controlled by the pilot. Fig 4 is the circuit diagram for the electronics on board the plane.

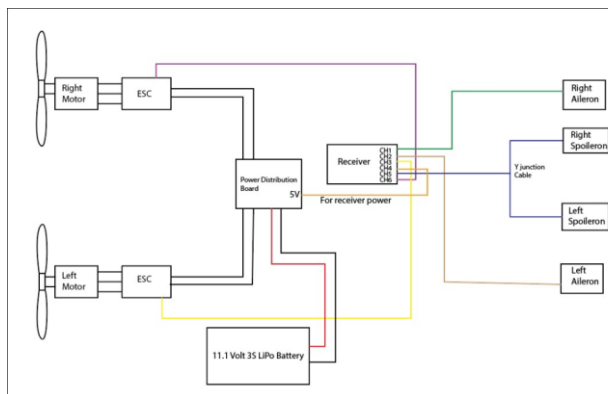


Fig. 4. Circuit diagram for the electronics on board the plane

The controls for the aircraft can be programmed, tuned and mixed using the transmitter. The transmitter has the feature of enabling differential thrust. Using this, the speed of each motor can be controlled independently, allowing the pilot to even control the aircraft about the yaw axis. This feature is especially useful for underwater traversal.

In case an autonomous flight mission has to be planned, a flight controller board such as a Pixhawk can be programmed and connected to the aircraft. This allows us to enable autopilot features, like making the aircraft follow a predefined path.

Pixhawk has an on-board gyroscope sensor and a GPS module. The pilot can use these features for a more stable flight.

V. DESIGN

A. Design of airfoil

Airfoil Selection is done for a flying wing, which is essentially a tailless airplane. Horizontal stabilizers are absent in such airplanes. These make them more susceptible to instability during take-off and landing due to factors like wind gusts. Airfoils in conventional airplanes produce a pitching moment (C_m) or a nose down effect. For a tailless airplane such airfoils may make it unstable as there is no horizontal

stabilizer to counter this effect. A reflexed airfoil may be used to counter this pitching moment. Reflexed airfoils have their trailing edge turned slightly upwards to provide more stability. Therefore, MH60 airfoil is used for this flying wing due to its aerodynamic characteristics.

As mentioned above, multiple parameters were considered in the selection of an air foil. Based on the flight dynamics and functional parameters, the airfoil MH60 was chosen for the wings. Fig 5. shows the airfoil design has, with its properties.

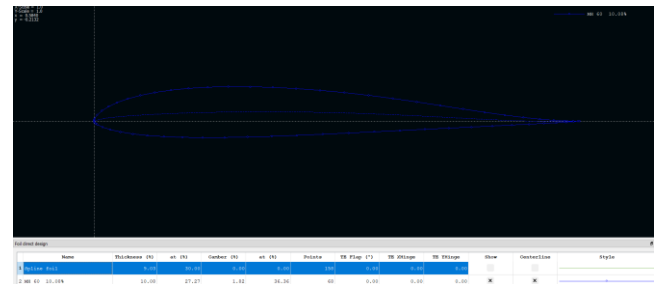


Fig. 5. Airfoil diagram plotted through data points in XFLR5

To further facilitate better dynamic stability over a wide range of Reynolds number, a flap was added to the trailing edge of the foil. A flap of + and - 5 degrees was included. Further analysis was performed on these foils to learn their effect and choose the best option. Fig 6. and Fig 7. show the + and -5 degree flap while Fig 8. shows the interface.

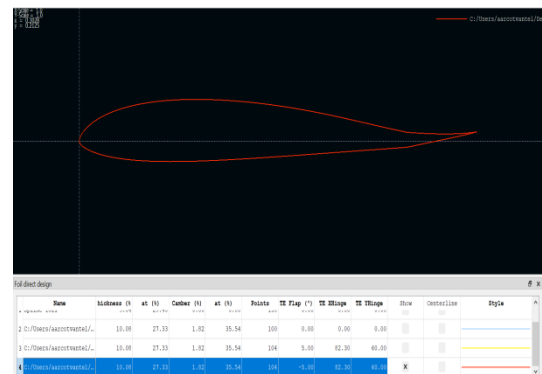


Fig. 6. Chosen airfoil with a negative angle flap

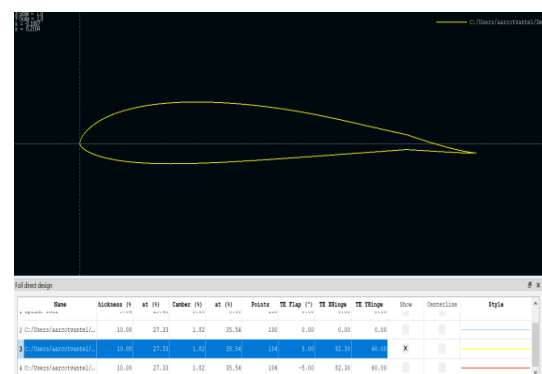


Fig. 7. Chosen airfoil with a positive angle flap

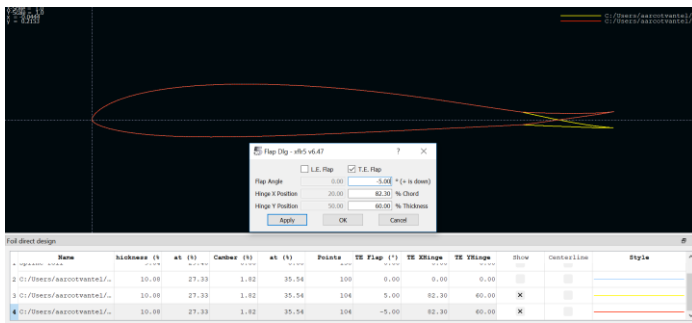


Fig. 8. Interface to set flap angle and location

1) *Flap comparison*: Including a flap increases the stability of a flying win UAV. Thus, multiple iterations are run for different angles of the flap. An upper angle flap of 5 degrees was found to be ideal for the functioning Reynolds range. The aforementioned comparisons can be observed in Fig 9.

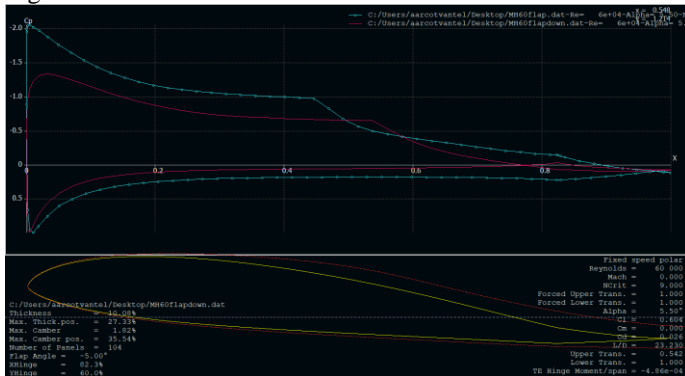


Fig. 9. Comparison of flaps through a graph plotted between C_p and Root Chord Length

Compared to a flap which is angled downwards, it can be observed that the separation of flow occurs earlier and loses stability earlier.

B. Airfoil analysis

Air foil – MH60

Dimensions: Max thickness – 10.1% at 26.9% chord; Max camber – 1.7% at 36.6% chord.

In order to observe its behaviour during flight a multi thread batch analysis is performed. A multi thread batch analysis basically helps in controlling the number of cores of the computer used while also aiding analysis of multiple foils.

In order to understand the effect of foil in flight, five major graphs are observed.

- C_L vs C_D
- C_L vs Alpha
- C_m vs Alpha
- C_L/C_D vs Alpha
- C_p vs X (chord)

A thorough understanding of these graphs helps in identifying the range of Reynolds number where the air foil

functions optimally and the range of angle of attack (AOA) where there is no separation of flow.

1) C_L vs C_D : The graph shown in Fig 10. is plotted between the coefficient of lift and coefficient of drag. Each line corresponds to the performance of foil within the specified Reynolds number. The first line begins at Re 10,000 and the final line corresponds to Re 2,000,000. Reading this graph gives us an understanding of the foils performance at specified Re and gives an insight into the operating range of the foil. Thus, helping us understand whether the chosen air foil is suitable for our needs.

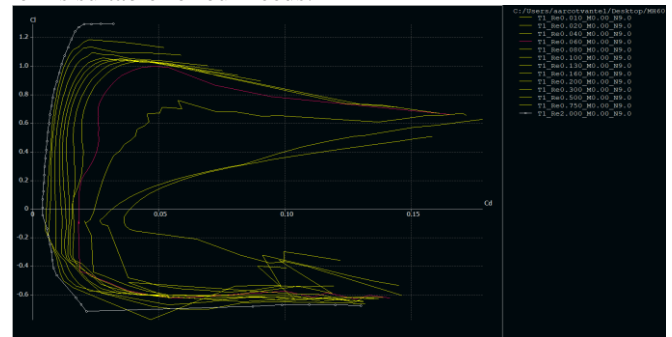


Fig. 10. Resultant graph plotted between coefficient of lift and coefficient of drag

2) C_L vs α : Coefficient of lift vs α i.e. angle of attack (AoA) graph plots the amount of lift gained by the UAV at varying angle of attacks and Reynolds number. This shows us the critical angle of attack and the behaviour of it at a specified Reynolds number. Fig 11. shows the plotted graph between C_L and α .

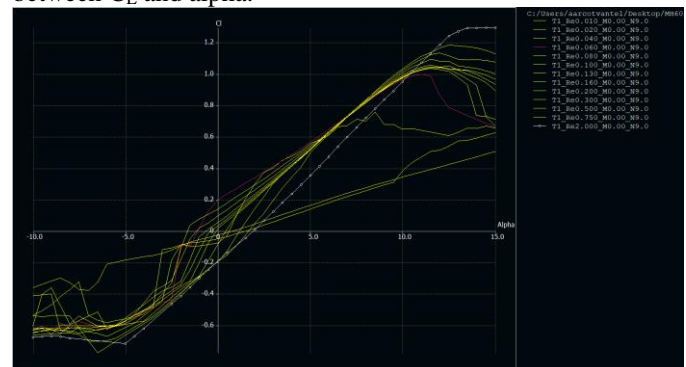


Fig. 11. Resultant graph plotted between coefficient of lift and angle of attack

3) C_m vs α : The graph in Fig 12. is plotted between the coefficient of moment and angle of attack, α . The graph helps in understanding the effects of a certain angle of attack to the moment of the airplane or in this case the UAV. The values are observed within a specified range of Reynolds Number.

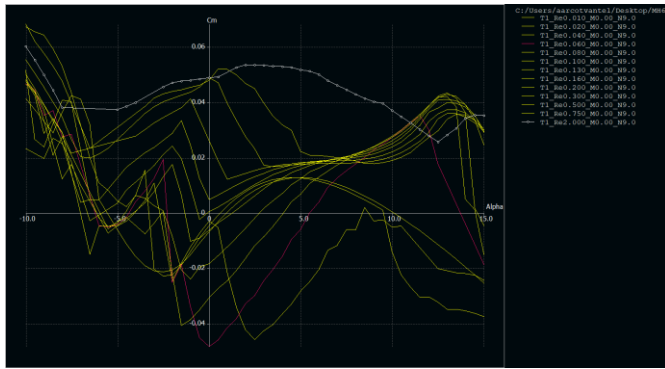


Fig. 12. Resultant graph plotted between coefficient of moment and angle of attack

4) C_L/C_D vs α : The lift to drag ratio versus α explains the flight economy i.e. the amount of drag incurred to lift gained. A higher lift to drag ratio corresponds to higher lift to corresponding drag, which is suitable in our case. From the graph in Fig 13. it can be seen that as the AoA increases, the L/D ratio increase, but it eventually reaches a critical point before falling. Comparing multiple graphs, a suitable AoA can be chosen.

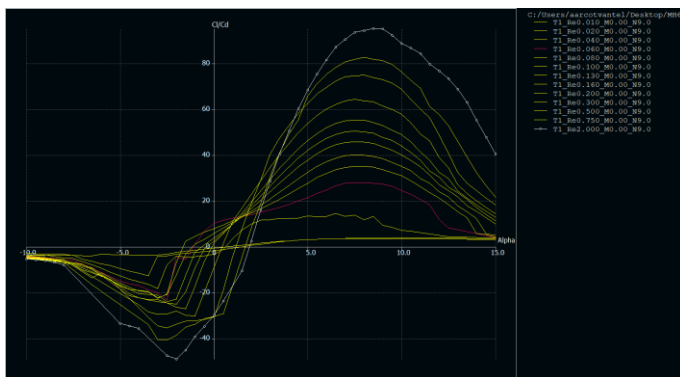


Fig. 13. Resultant graph plotted between lift-drag ratio and angle of attack

5) C_p vs X : Fig 14. is the graph plotted between coefficient of pressure and root chord length (X). The bump in the slope is the separation of flow at that particular length of chord. If separation is observed at a point close to the head of the UAV, the stability in flight is reduced.

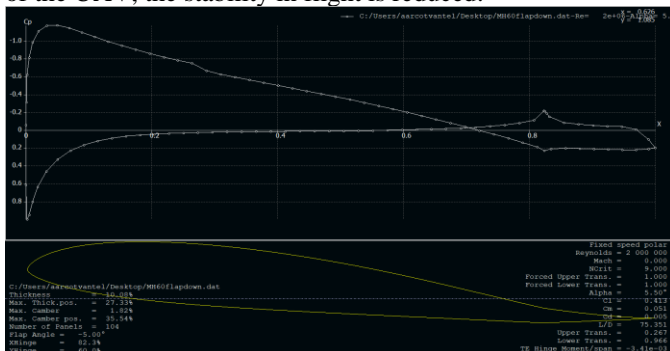


Fig. 14. Resultant graph plotted between coefficient of pressure and Root Chord Length

C. Wing design

After thorough analysis of the foil, determining its operating range and the right AoA for required application, the wing design is begun. Wing design includes designing of the flying wing connected to the main body. The software XFLR5 is used for this purpose.

The dimensions of the wing were determined initially through wing cube loading.

As seen in Fig 15, the data of chord length, span, sweep angle, dihedral angle and twist are determined. Through adding multiple sections, winglets are also included.

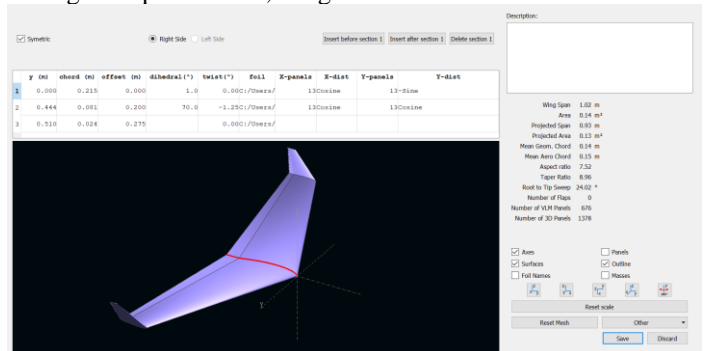


Fig. 15. Wing design parameters and its dimensions

1) *Empennage design*: Empennage design is the design of horizontal and vertical stabilizers with due consideration for lateral and longitudinal stability. As the name suggests, stabilizers effect the stability of the UAV, both lateral and longitudinal, in flight. The stability performance is defined in further detail in section 5.6. These dimensions are defined after thorough analysis through iterations and introduced as flaps into the foil. Being a fixed wing there are no elevators and fins thus, an aileron is used for horizontal stabilizers.

Winglets are used as vertical stabilizers in this flying wing UAV. The winglet is of blended type with an angular transition. Final dimensions of these stabilizers are mentioned in section 7.

D. Design of body

The wing body contains the major components of the airplane. The components are battery, ESC, wiring, pixhawk and extra weights to balance the centre of gravity. Dimensions of the wing body depend on the dimensions of the listed components. The largest dimensions are of the battery, so the design is based around it. A CAD model from the resulting wing and body design with a few required modifications for the wing body was modeled on SOLIDWORKS. Fig 16, 17, 18 and 19 show the stages and views of design.

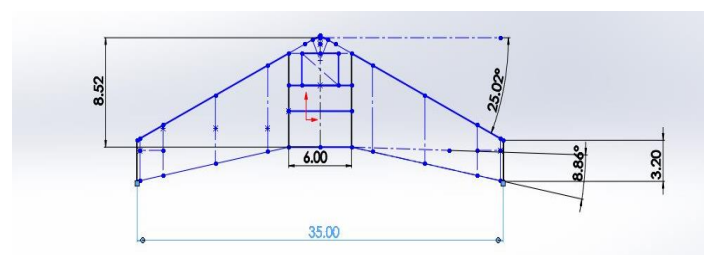


Fig. 16. 2D view of the UAV and its design dimensions

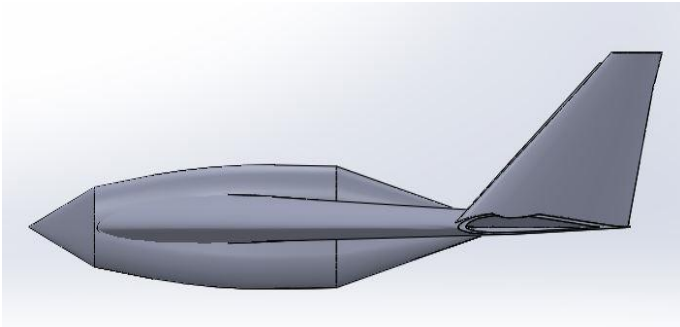


Fig. 17. Side profile view of flying wing design

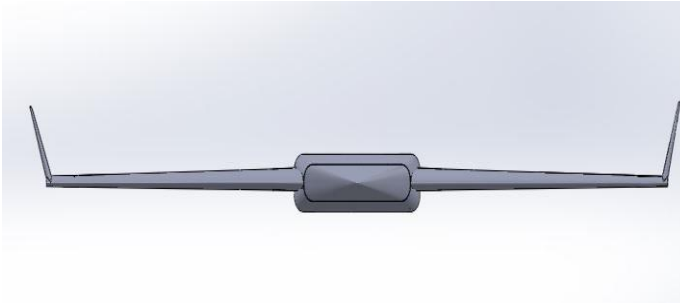


Fig. 18. Front view of flying wing design

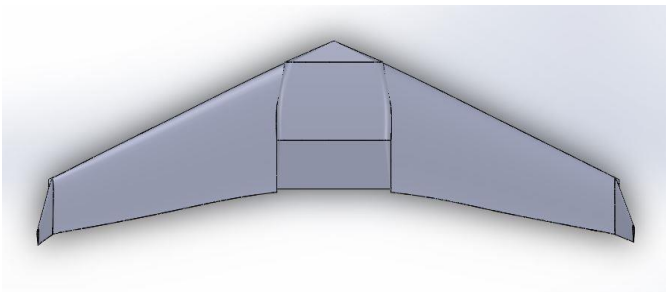


Fig. 19. Top view of flying wing design

Final dimensions of wing and body are mentioned in section 7.

E. Performance analysis

After the design and analysis of selected air foil and design of wing is completed, a performance analysis on the wing is performed. This performance analysis gives results on the functioning of specified wing under required conditions and is also required to perform a stability analysis on the wing and determine its static and dynamic stability.

The performance analysis also serves as point of comparison between the UAV's performance ,above and under water. There are multiple types of polars and analysis methods to be chosen from in order to perform a performance analysis. Fig 20 and 21 show the interface for polar types and analysis methods.

Polar types

- Type 1 – fixed speed
- Type 2 – fixed lift
- Type 3 – fixed AoA
- Type 4 – beta range

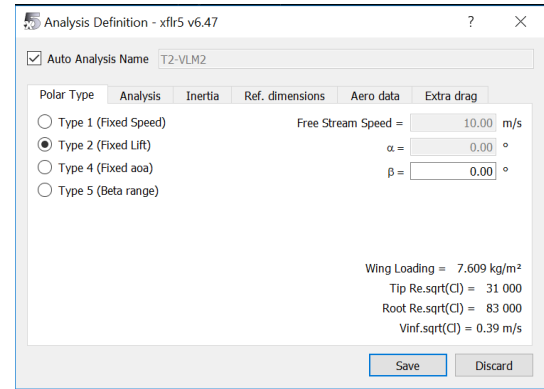


Fig. 20. Types of polars for performance analysis

Analysis methods

- LLT (wing only)
- Horseshoe vortex (VLM1)
- Ring vortex VLM2
- 3D panels

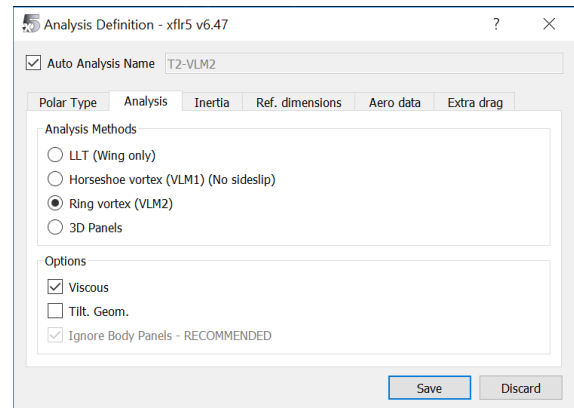


Fig. 21. Types of analysis methods for performance analysis

Based on our requirements, the type of analysis being performed, and the results need, the following settings were chosen.

Type 2, Ring vortex VLM2

Performing the analysis provides parameters such as

- Coefficient of pressure
- Lift
- Induced drag
- Surface velocity
- Moment
- Viscous drag
- Downwash
- Stream

From the above results we concentrate on the lift, drag, moment and lift to drag ratio. These parameters are then plotted against angle of attack and lift. The plotted graph helps us understand the wings performance.

The results were plotted for both above and under water performance and can be observed in Fig 22.

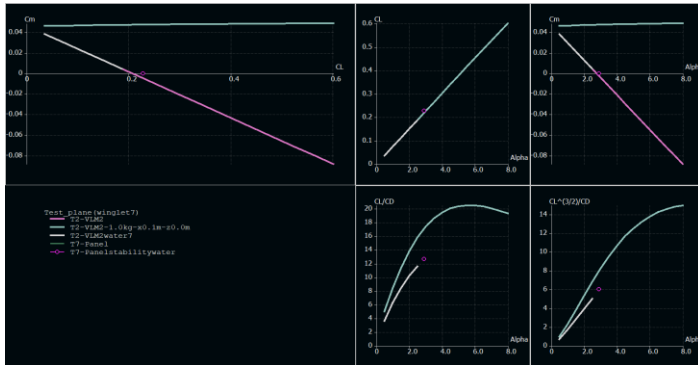


Fig. 22. Resultant graph comparing dynamic flight performance results above and under water

The above graph depicts the performance of a wing and compares above water performance to underwater performance.

Most results coincide well with each other, except for lift to drag ratio and drag polar. This is expected as there is a change in density and kinematic viscosity of the two operating environments.

The results for fixed lift polar type was computed for travel in air as well as water. Here the lift of the flight is held constant while the AOA changes, the lift fixed lift is compensated by the change in velocity.

The figures below from Fig 23 to Fig 33 below depict how wing and body move in air and water by comparing lift gradient, viscous drag, pressure gradient and streamlines for air at angle of attack- 2.5,0deg and water at angle of attack 2.5deg.

With the decrease in Angle of Attack, to maintain the same lift the velocity is increased thus increasing the drag on the plane wing and body. This can be seen with the high viscous drag at AOA 0 which compared to AOA 2.5 is higher.

In contrast, the viscous drag in water when compared to air at the same AOA is high with a lower velocity. This is due to the high pressure underwater and the high density of water.

1) Lift gradient

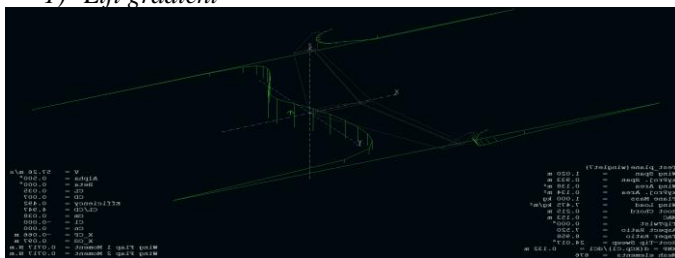


Fig. 23. Lift gradient at 0 degrees angle of attack

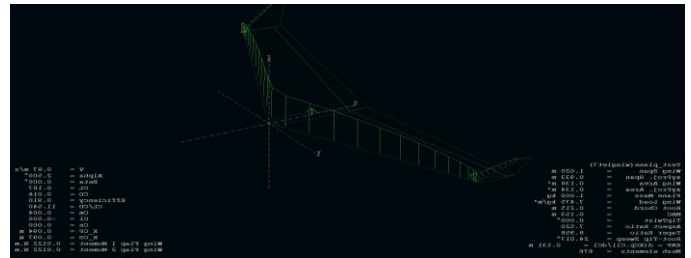


Fig. 24. Lift gradient at 2.5 degrees angle of attack

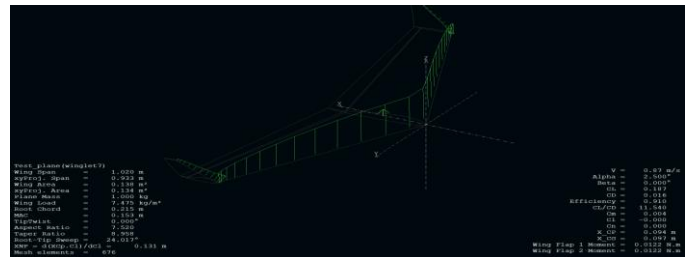


Fig. 25. Lift gradient at 2.5 degrees angle of attack, underwater

2) Viscous drag

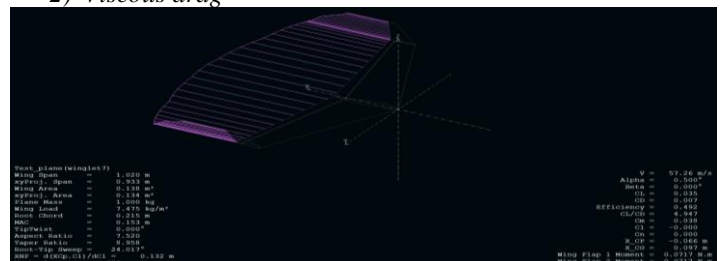


Fig. 26. Viscous drag at 0 degrees angle of attack

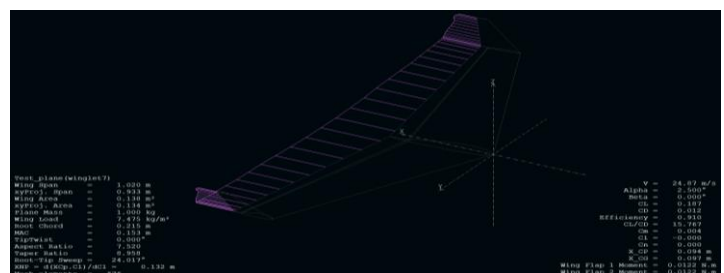


Fig. 27. Viscous drag at 2.5 degrees angle of attack

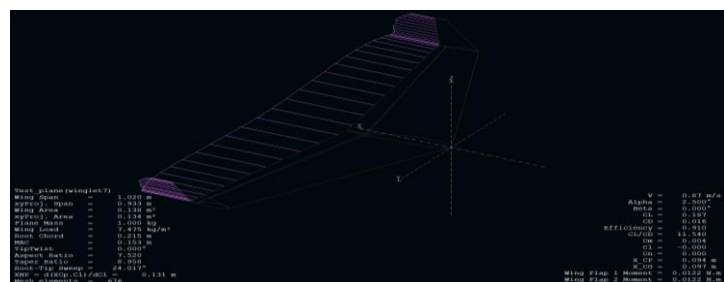
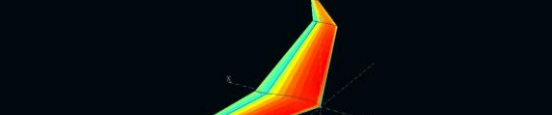


Fig. 28. Viscous drag at 2.5 degrees angle of attack, underwater

Wing Plan

Root plane	=	0.888 m
Wing Span	=	0.888 m
Symptol Span	=	0.888 m
Wing Area	=	0.131 m ²
Wing Area Root	=	0.132 m ²
Plane Mass	=	1.000 kg
Wing Load	=	1.016 kg/m ²
Nostr Chord	=	0.211 m
NAC	=	0.150 m
Tipwidth	=	0.000"
Aspect Ratio	=	8.000
Taper Ratio	=	0.650"
Nostr-Tip Sweep	=	20.554°
Use = distn cl/area	=	0.127 m
Mesh elements	=	338

V =	24.17 m/s
Alpha =	2.500°
Beta =	0.000°
CL	0.298
CD	0.012
Kfriction	1.045
CL/CD	17.827
CL	0.400
CD	0.040
K	0.002
X CG	-0.395 m
X CG	-0.049 m
Wing flap 1 Moment	-0.014 Nm
Wing flap 2 Moment	-0.014 Nm



Test_plane(wing1.pl)

Wing_Typ	=	3.020 m	V	=	57.26 m/s
Wing1.Span	=	0.923 m	Alpha	=	0.500°
Wing1.A	=	0.138 m	Mach	=	0.000
Wing1.Area	=	0.134 m²	CL	=	0.035
Plane_Mach	=	1.000 kg	CD	=	0.007
Wing_Load	=	7.475 kg/m²	Efficiency	=	0.492
Wing_Chord	=	0.215 m	CL/Cd	=	4.942
MAC	=	0.153 m	cm	=	0.038
WingTwist	=	0.900°	CI	=	0.000
Aspect_Ratio	=	7.520	Xcm	=	0.000
Reynolds_Ratio	=	0.958	X_CP	=	-0.048 m
Root-Tip Sweep	=	24.017°	X_CD	=	0.097 m
Repr = 0.020: 0.1/0.1	=	0.132 m	Wing Flap 1 Moment	=	0.0117 N.m
Wing elements	=	676	Wing Flap 2 Moment	=	0.0717 N.m

Test plane(wingintf)

wing Span	1.020 m
upFrontj.Span	0.933 m
wing Area	0.139 m ²
upFrontj.Area	0.134 m ²
planform Mass	1.000 kg
wing Load	7.475 kg/m ²
root Chord	0.215 m
tip	0.153 m
upFrontj	0.000 m
Aspect Ratio	7.520
Aspect Ratio	8.968
root-Tip Sweep	24.013°
root-Tip Sweep	0.122 m

Wing Flap 1

V	24.67 m/s
Alt	3.306 m
ReMa	8.000*
ReMa	1.197
CD	0.012
ReFrontj	1.910
CL/FCD	15.767
CI	-0.000
CI	-0.000
X_CP	0.984 m
W-CD	0.008 m
W-CD	0.012 m

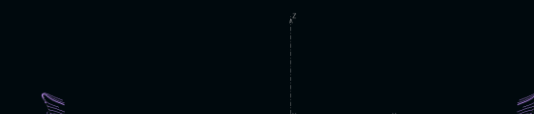
```

      cp
      0.25
      0.62
      0.76
      0.70
      0.63
      0.57
      0.54
      0.88
      0.21
      0.25
      0.39
      0.04
      0.03
      -0.01
      -0.33
      -0.07
      -0.20
      -0.28
      -0.39

      w = 0.95 m/s
      Alight = 0.5007
      rho = 1.204
      SFL = 0.107
      CxFL = 0.6
      Efficiency = 7.740
      Cw = 11.940
      Cx = -0.000
      Cy = 0.000
      Cx_Cyl = 0.004
      Cy_Cyl = 0.004

      Wing Plan 3 Moments = 0.0132 M
      Weight = 0.000 M

```



```

Test_plane(winglet?)
Wing Span      = 1.000 m
WingTip Span   = 0.900 m
Wing Area      = 0.186 m^2
WingTip Area   = 0.158 m^2
Plane Mass     = 1.000 kg
Wing Load      = 1.015 kg/m^2
Root Chord     = 0.215 m
Wing Chord     = 0.153 m
WingTip Chord  = 0.080 m
Aspect Ratio    = 1.500
WingTip Ratio  = 0.800
WingTip Sweep  = 24.019°
WingTip dX/dY, C11/C21 = 0.132 n
Mesh elements  = 676
  
```

V = 24.87 m/s
 Alpha = 2.500°
 beta = 0.000°
 CL = 0.187
 CD = 0.012
 efficiency = 0.910
 cL/cD = 76.767
 Cm = 0.004
 Cn = 0.000
 Cx = 0.004
 Cy = 0.097 m
 Wing Flap Moment = 0.0122 N.m
 Wing Flap Moment = 0.0122 N.m

1) *Cm vs alpha*: As seen in Fig 34, the curve has a negative slope. The value of angle of attack where the moment is zero is also a good value for the angle of attack for the wing.

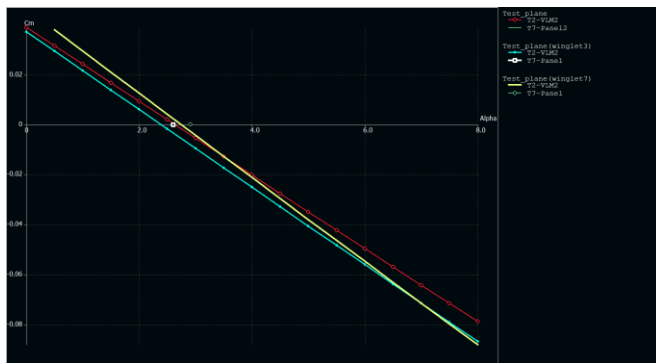


Fig. 34. Graph between coefficient of moment and angle of attack

2) C_m vs C_L : At zero moment the lift is positive. This confirms the prerequisites. Fig 35 shows the graph plotted between C_m and C_L .

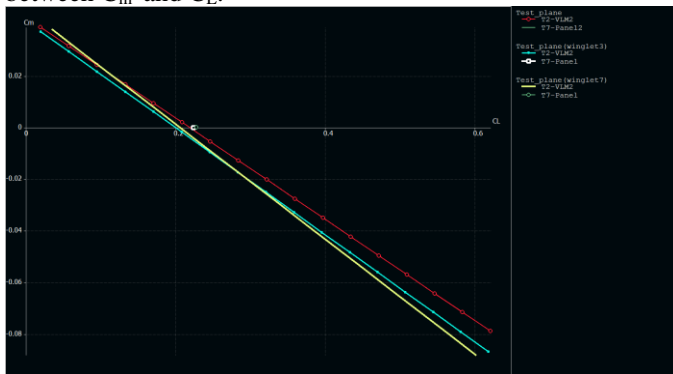


Fig. 35. Graph between coefficient of moment and coefficient of lift

3) *Centre of Gravity*: To determine the centre of gravity we first determine the neutral point (NP). The NP is a point on the plane where the moment is independent of lift. The centre of gravity is then determined to be within 15% to 25% of the specified neutral point.

The neutral point is determined by alternating the centre of gravity until the curve is approximately horizontal to the x axis.

Later the masses are accordingly positioned on the plane body to gain the centre of gravity at the determined point. This weight positioning interface is shown in Fig 37. while Fig 38 shows a three dimensional view of the weight distribution.

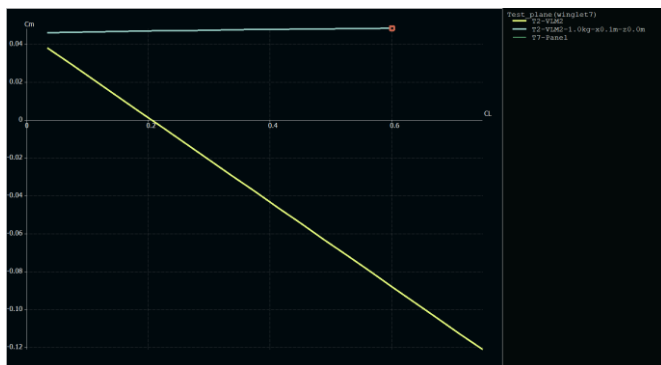


Fig. 36. Graph between coefficient of moment and coefficient of lift to determine neutral point.

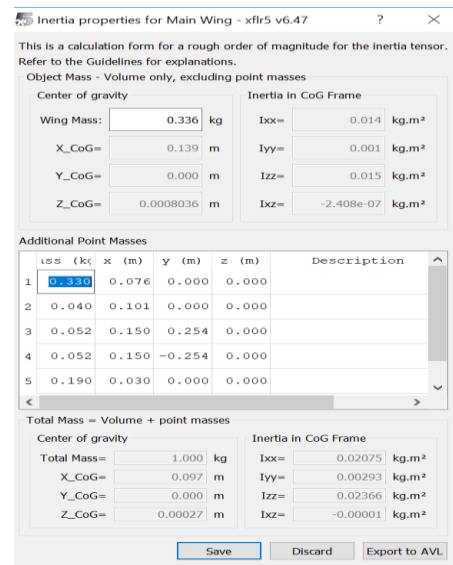


Fig. 37. Mass distribution and centre of gravity

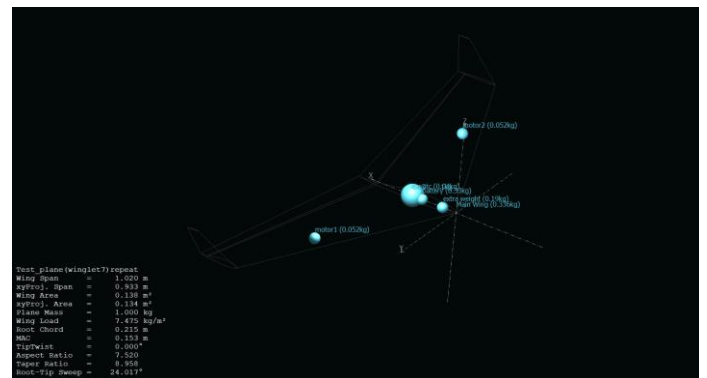


Fig. 38. 3D view of the mass distribution within the UAV

G. Ingress and egress mechanism

1) *Launching*: The wing can be launched with hand or can be launched using a bungee catapult launcher during take-off.

2) *Ingress/egress mechanism*: The flying wing has open wingtips, and the wing has an inner cavity. The wing acts as a ballast tank. When the wing has to traverse underwater, it first has to land on the water surface. Water enters the wing through the open wingtip and fills up the wing. This makes the wing less buoyant and can ingress underwater by pitching downward and propelling.

The two motors present on the wing make it easier to thrust inward and the differential thrust mechanism makes it easier to make turns. But, more than 10% of the capacity of the motor should not be used, as the ESC would be insulated underwater and there may be a risk of it burning out.

During egress from the water body, the wing has to propel out at a high velocity and the spoilers are opened to drain out the water, making it lighter for aerial flight. The spoilers are then closed once the UAV enters aerial flight. Fig 39 and Fig 40 show a sectional view of the acting ballast for ingress.

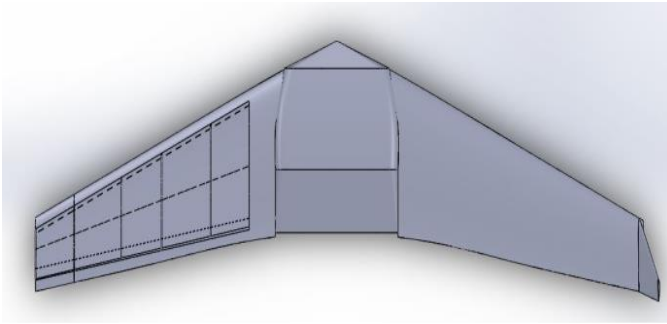


Fig. 39. Inner sectional view of wing depicting the catchment area of flooding

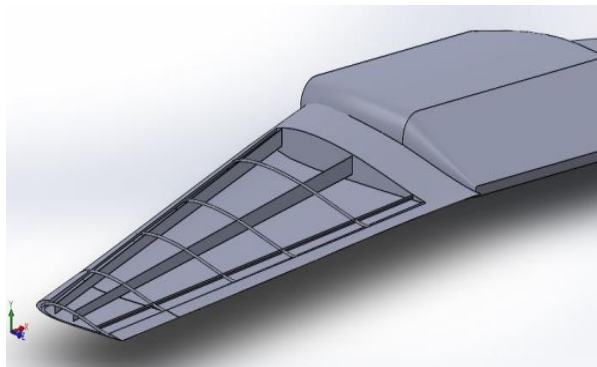


Fig. 40. Hollow wing to enable flooding for ingress

H. Static structural analysis

A wing structure consists of multiple layers. The outer layer consists of a hard casing that forms the outer curved section of the wing, while the inner sections contain support structures called spars and ribs. These structures work like iron rods installed within concrete pillars. They provide structural stability and strength to the wing.

Failure of these structures can cause failure of the whole wing, therefore performing an analysis on them is necessary. Here analysis is only performed on the spars as these structures support all the loads. A static structural analysis is performed on them and the material chosen is mentioned below.

Boundary Conditions: The spars run from one end of the body to the tip of the wing i.e. the tip chord. The center of gravity rests within the body i.e. most of the weights rest within this structure. As a result, the body is treated as a fixed support while the other end is treated as a free end. This is a cantilever beam and accordingly analysis is performed on them.

Loading Conditions: A 75 N force is applied on the other end in the downward direction, making it a cantilever beam. This is to simulate 3g forces experienced by the spar while supporting the flying wing during takeoff, cruising, touchdown and underwater traversal. (The weight of the flying wing is 1 kg (10 N).

Tables I, II and III specify the material properties, design dimensions and mesh properties respectively.

TABLE I. MATERIAL TYPE AND ITS PROPERTIES

Material properties	Values
Material	Carbon fiber composite
Density	1.8 g/cc
Young's Modulus	70 Gpa
Poisson's ratio	0.3

TABLE II. SPAR DIMENSIONS

Dimension	Values
Length	17 in
Width	2mm

TABLE III. MESH STATISTICS AND PROPERTIES

Mesh properties	Values
Mesh type	2D mesh
Element size	4mm
Number of nodes	27917
Number of elements	4370

VI. PROTOTYPE

With the values from the analysis and resulting wing and body design the final CAD prototype was modeled on SOLIDWORKS.

Material selection is important for any vehicle or drone, it has to satisfy the design requirements at the same time hold up to the factors such as cost and availability. There is a plethora of material available that meet all the requirements from the design and fabrication point of view. We look to the market of existing drones and underwater UAVs for a lead and have benchmarked a few materials. The material we finally chose was Carbon Fiber composite.

The final CAD prototype is an assembly of all the components mentioned arranged in the plane body including rotors. Fig 41 to Fig 44 show the CAD models and final rendered prototypes of the UAV.

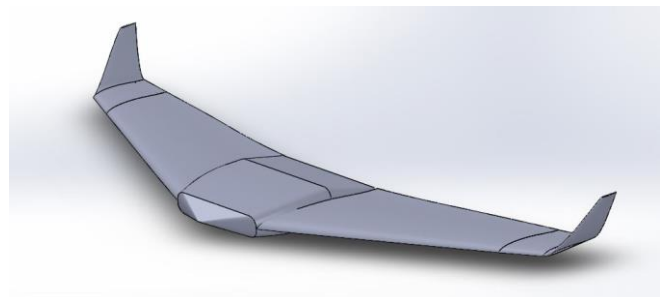


Fig. 41. Isometric view of final wing and body design



Fig. 42. Isometric view of rendered prototype



Fig. 43. Front view of rendered prototype

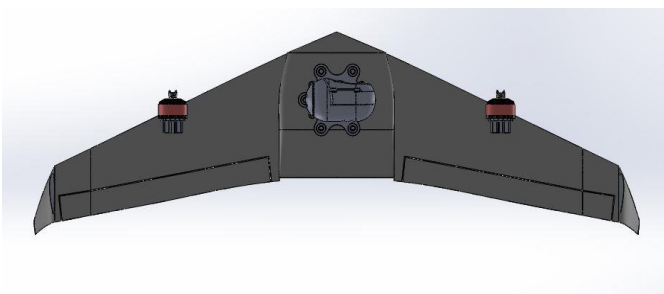


Fig. 44. Bottom view of final prototype

A. Figures and Tables

1) *Positioning Figures and Tables:* Place figures and tables at the top and bottom of columns. Avoid placing them in the middle of columns. Large figures and tables may span across both columns. Figure captions should be below the figures; table heads should appear above the tables. Insert figures and tables after they are cited in the text. Use the abbreviation "Fig. 1," even at the beginning of a sentence.

We suggest that you use a text box to insert a graphic (which is ideally a 300 dpi resolution TIFF or EPS file with all fonts embedded) because this method is somewhat more stable than directly inserting a picture.

To have non-visible rules on your frame, use the MSWord "Format" pull-down menu, select Text Box > Colors and Lines to choose No Fill and No Line.

TABLE IV. TABLE STYLES

Table Head	Table Column Head		
	Table column subhead	Subhead	Subhead
copy	More table copy ^a		

^a. Sample of a Table footnote. (Table footnote)

b.

Fig. 45. Example of a figure caption. (figure caption)

Figure Labels: Use 8 point Times New Roman for Figure labels. Use words rather than symbols or abbreviations when writing Figure axis labels to avoid confusing the reader. As an example, write the quantity "Magnetization," or "Magnetization, M," not just "M." If including units in the label, present them within parentheses. Do not label axes only with units. In the example, write "Magnetization (A/m)" or "Magnetization (A (m(1)," not just "A/m." Do not label axes with a ratio of quantities and units. For example, write "Temperature (K)," not "Temperature/K."

ACKNOWLEDGMENT

The preferred spelling of the word "acknowledgment" in America is without an "e" after the "g." Avoid the stilted expression "one of us (R. B. G.) thanks ...". Instead, try "R. B. G. thanks...". Put sponsor acknowledgments in the unnumbered footnote on the first page.

REFERENCES

The template will number citations consecutively within brackets [1]. The sentence punctuation follows the bracket [2]. Refer simply to the reference number, as in [3]—do not use "Ref. [3]" or "reference [3]" except at the beginning of a sentence: "Reference [3] was the first ..."

Number footnotes separately in superscripts. Place the actual footnote at the bottom of the column in which it was cited. Do not put footnotes in the reference list. Use letters for table footnotes.

Unless there are six authors or more give all authors' names; do not use "et al.". Papers that have not been published, even if they have been submitted for publication, should be cited as "unpublished" [4]. Papers that have been accepted for publication should be cited as "in press" [5]. Capitalize only the first word in a paper title, except for proper nouns and element symbols.

For papers published in translation journals, please give the English citation first, followed by the original foreign-language citation [6].

- [1] G. Eason, B. Noble, and I.N. Sneddon, "On certain integrals of Lipschitz-Hankel type involving products of Bessel functions," Phil. Trans. Roy. Soc. London, vol. A247, pp. 529-551, April 1955. (references)
- [2] J. Clerk Maxwell, A Treatise on Electricity and Magnetism, 3rd ed., vol. 2. Oxford: Clarendon, 1892, pp.68-73.
- [3] I.S. Jacobs and C.P. Bean, "Fine particles, thin films and exchange anisotropy," in Magnetism, vol. III, G.T. Rado and H. Suhl, Eds. New York: Academic, 1963, pp. 271-350.
- [4] K. Elissa, "Title of paper if known," unpublished.

- [5] R. Nicole, "Title of paper with only first word capitalized," J. Name Stand. Abbrev., in press.
- [6] Y. Yorozu, M. Hirano, K. Oka, and Y. Tagawa, "Electron spectroscopy studies on magneto-optical media and plastic substrate interface," IEEE Transl. J. Magn. Japan, vol. 2, pp. 740-741, August 1987 [Digests 9th Annual Conf. Magnetism Japan, p. 301, 1982].
- [7] M. Young, The Technical Writer's Handbook. Mill Valley, CA: University Science, 1989.